

## Nucleosome sliding can influence the spreading of histone modifications

Shantanu Kadam,<sup>1,\*</sup> Tripti Bameta,<sup>2,†</sup> and Ranjith Padinhateeri<sup>1,‡</sup>

<sup>1</sup>*Department of Biosciences and Bioengineering, Indian Institute of Technology Bombay, Mumbai 400076, India*

<sup>2</sup>*Department of Medical Oncology, Tata Memorial Centre, Homi Bhabha National Institute, Mumbai 410210, India*



(Received 14 October 2021; accepted 25 July 2022; published 16 August 2022)

Nucleosomes are the fundamental building blocks of chromatin that not only help in the folding of chromatin, but also in carrying epigenetic information. It is known that nucleosome sliding is responsible for dynamically organizing chromatin structure and the resulting gene regulation. Since sliding can move two neighboring nucleosomes physically close or away, can it play a role in the spreading of histone modifications? We investigate this by simulating a stochastic model that couples nucleosome dynamics with the kinetics of histone modifications. We show that the sliding of nucleosomes can affect the modification pattern as well as the time it takes to modify a given region of chromatin. Exploring different nucleosome densities and modification kinetic parameters, we show that nucleosome sliding can be important for creating histone modification domains. Our model predicts that nucleosome density coupled with sliding dynamics can create an asymmetric histone modification profile around regulatory regions. We also compute the probability distribution of modified nucleosomes and relaxation kinetics of modifications. Our predictions are comparable with known experimental results.

DOI: [10.1103/PhysRevE.106.024408](https://doi.org/10.1103/PhysRevE.106.024408)

### I. INTRODUCTION

In cells, DNA is folded and wrapped around octamers of histone proteins forming an array of nucleosomes. The nucleosome is considered to be the fundamental repeating unit of chromatin, and its positioning is important for gene regulation. In typical chromatin, two neighboring nucleosomes are separated by short segments of linker DNA of lengths ranging from 10 to 60 bp [1–4]. Recent advancements in experimental and computational methods have helped us to understand how nucleosomes are organized along DNA [5–21].

Nucleosomes also carry epigenetic information in the form of histone modifications apart from the folding of chromatin. Specific amino acid residues of histone proteins carry chemical modifications, such as methylation and acetylations as histone marks [1,2]. At specified locations on each histone protein, certain enzymes add or remove relevant chemical groups leading to a pattern of post-translational modifications along the chromatin contour [22,23]. How these marks get organized along the chromatin is crucial for regulating cellular processes, such as gene expression, DNA repair, DNA replication, etc. [24–28]. Experimentally, one can measure the pattern of histone modification at a given instant in a population of cells by the ChIP-Seq methods [29,30]. However, it is a difficult task to measure the modification dynamics in individual cells in real time [31–33]. Moreover, comprehensive mechanisms that leads to dynamic histone modification patterns are not fully understood yet.

The phenomena of spreading and subsequent maintenance of histone modifications have been experimentally studied with great interest. Several studies [34–37] have investigated the formation of heterochromatin and epigenetic inheritance. In these studies, the modified nucleosomes recruit enzymes to similarly modify neighboring unmodified nucleosomes based on a linear stepwise process. Also, there are studies where researchers have tried to unravel how histone modifications spread along chromatin fiber from a given initiation site [38,39]. All these studies have contributed considerably to the understanding of modification spreading.

Several theoretical models [4,24,40] have been developed to provide insights into the dynamics of histone modifications. Over the years, Dodd *et al.* [41], Sneppen *et al.* [42], Dodd and Sneppen [43], and Obersriebnig *et al.* [44] have developed models that explain different aspects of histone modification spreading and inheritance. They have proposed that long-range interactions lead to a bistable paradigm for a certain range of parameters. Hathaway *et al.* proposed a linear propagation scheme to explain patterns in H3K9me3 that involved localized peaks and soft borders of heterochromatic islands [45]. In their model [45], they incorporated nucleation, propagation, and turnover rates for modifications, which were necessary to describe H3K9me3 domains. In a separate work, they extended the model to estimate several dynamic quantities predicting domain sizes for different values of rates [46]. This standard model was also extended to incorporate spreading beyond nearest neighbors. There are also other stochastic models [47,48] that include recruitment, diffusion, and long-range interactions leading to the formation of modification patterns. There has also been a Potts-type model by Zhang *et al.* [49], stressing the local nature of interactions, and a model introduced by Binder *et al.* [50] investigating epigenetic silencing in eukaryotes. Another set

\*shantanurk123@gmail.com

†tbameta@actrec.gov.in

‡ranjithp@iitb.ac.in

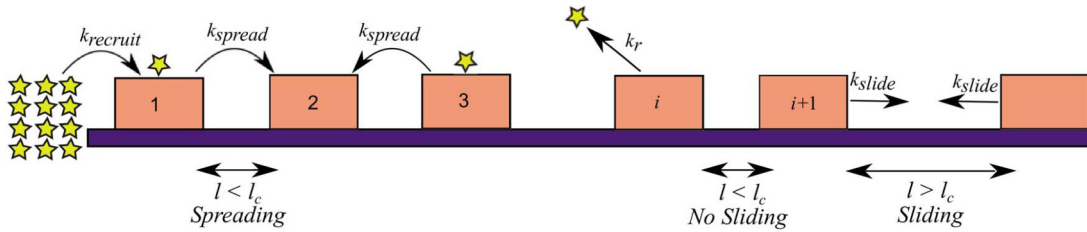


FIG. 1. Schematic of the model: Histone modifying enzymes (“writers”) are recruited with a rate  $k_{\text{recruit}}$  at the left boundary. The spreading of the modification (yellow star) occurs with a rate  $k_{\text{spread}}$  when the distance between two neighboring nucleosomes (brown blocks) is less than  $l_c$ . The demodification of a nucleosome occurs randomly with a rate  $k_r$  at any modified nucleosome. The sliding of a nucleosome occurs with a rate  $k_{\text{slide}}$  with a step size of 10 bp, provided that there is a free linker DNA space  $\geq l_c$  to slide. We take  $l_c = 10$  bp in this paper.

of models explicitly account for three-dimensional (3D) looping and investigate the role of looping in the spreading of histone modifications [51–57]. In these models, the coupling of 3D configurations with spreadings of histone modifications is investigated.

Nearly all the modeling studies have assumed that nucleosomes are static and modifications can spread to the nearest neighbor nucleosomes independent of the distance between them. It is plausible that two neighboring nucleosomes are far from one another, and the spreading may get hindered due to the large gap between those nucleosomes [58,59]. One way two neighboring nucleosomes can regulate the gap—internucleosomal distance or linker length—is via sliding of nucleosomes [60–65]. None of the existing models account for the role of the sliding of nucleosomes in the context of modification spreading. In this paper, we propose a stochastic model to study the spreading and maintenance of histone modifications taking into account the role of nucleosome sliding.

In our model, we have included sliding of nucleosomes (due to remodeling complexes), modification of nucleosomes (by modification enzymes), and removal of a modification mark (by demodifying enzymes) as kinetic events accompanied by their respective rates. We aim to determine whether nucleosome sliding events play any kind of role in spreading the modifications in a particular genomic region, and how sliding could couple with nucleosome density to determine the modification dynamics.

We have organized this article as follows: First, we have explained the features associated with our one-dimensional (1D) model along with simulation details. In the results section, first, we have studied the variation of mean modification spreading times (MMSTs) for different sliding rates and demodification rates. In the next section, we have computed probabilities of modified nucleosomes at two different nucleosome densities and compared them with existing experimental results. We have studied the dynamics of modified nucleosomes by estimating their statistical quantities. In the last section, the relaxation dynamics of modified nucleosomes are reported and their behavior analyzed. Finally, we have provided the conclusions drawn from our paper along with some suggestions for new experiments to test our predictions.

## II. MODEL

This section describes the model (see Fig. 1) that we use in our simulations. We have modeled the spreading of

modifications in a quantitative way by simplifying the 3D structure of DNA and focusing on a small section of DNA taking it as a 1D lattice. Thus, in the model, the DNA is considered as a 1D lattice (violet bar) of length  $L = 5000$  bp. The nucleosomes (brown rectangular blocks) with indices  $i = 1, 2, \dots, N$  on the DNA are modeled as hard-core particles with each one occupying  $k = 147$  bp along the lattice. The hard-core steric interactions among the nucleosomes are modeled by prohibiting a lattice site from getting occupied simultaneously by more than one nucleosome.

In the model, we have considered four kinetic events: (i) recruitment of modification enzymes with a rate  $k_{\text{recruit}}$ , (ii) transfer of this modification enzyme to an unmodified nucleosome with a rate  $k_{\text{spread}}$ , (iii) fall of modification enzyme with a rate  $k_r$ , and (iv) sliding of nucleosomes along the DNA with a rate  $k_{\text{slide}}$ . In this paper, the binding and dissociation of nucleosomes are ignored. Hence, we have assumed that the total number of nucleosomes ( $N$ ) is constant.

It is reported that Refs. [39,47,51] for a genomic or a promoter region recruitment of enzymes could be performed either to the left or the right side. The enzymes bind to the sites, which corresponds to a nucleosome free region (3′ or 5′ NFR). These binding (initiation and recruitment) sites can either correspond to a nucleosome located at the center of the lattice or at the left or right boundary. In our case, we consider a situation where modification enzymes are recruited at a specific location  $i = 0$  (left end of the lattice) with a rate  $k_{\text{recruit}}$  (Fig. 1). This is implemented when the nucleosome ( $i = 1$ ) gets closer to the source of the modification enzymes within a distance (gap between two nucleosomes) less than  $l_c = 10$  bp. We took 10 bp because it is often found that nucleosome slides in units of 10 bp. The experimental study where nucleosome-remodeling factor nucleosome remodeling factor slides the nucleosome in the units of 10 bp [66]; whereas studies which consider 10 bp periodicities of dinucleotides along the nucleosome length have led us to take  $l_c = 10$  bp [67,68]. The recruited modification enzyme further spreads along the lattice with a rate  $k_{\text{spread}}$  to a neighboring unmodified nucleosome, provided the internucleosomal distance is less than  $l_c = 10$  bp. One of the hallmarks of histone modification spreading is the positive feedback [41,51]. In this model, a modified nucleosome, inducing modification to a spatially close ( $\leq 10$  bp) neighbor, is essentially the positive feedback. In the simulations, it is assumed that the rate of recruitment ( $k_{\text{recruit}}$ ) is the same as the rate of spreading ( $k_{\text{spread}}$ ). The modified nucleosome can be randomly demodified by removal

of the modification enzyme with a rate  $k_r$ . Our simulations aim to answer the following question: How does nucleosome sliding affect the spreading of histone modifications? Hence, we incorporated random nucleosome sliding to the left or right with a rate  $k_{\text{slide}}$  per nucleosome. This rate represents the rate of reaction by ATP-dependent chromatin remodelers [69] that are responsible for such repositioning of nucleosomes in cells. It is assumed that sliding step size is 10 bp such that the diffusion constant is  $\sim k_{\text{slide}} (10 \text{ bp})^2$  [5,66]. In the studies, it is assumed that beyond  $i = 1$  and  $i = N$  there are boundary elements, which do not allow the spreading any further.

We performed kinetic Monte Carlo simulations using Doob-Gillespie algorithm [70–73] using the rates of sliding, modification, and demodification events. All these events are independent of each other. In this way, the simulation was run for some desired time. The nucleosome density is calculated as  $\rho = \frac{147 * N}{L}$ , where  $N$  is the total number of nucleosomes, and  $L$  is the total length of the 1D lattice. In all the simulations discussed in this paper, the modification rate  $k_{\text{spread}}$  is kept fixed at  $1 \text{ s}^{-1}$ . The rates ( $k_{\text{slide}}$ ,  $k_r$ ) of all other events are scaled with  $k_{\text{spread}}$  giving dimensionless quantities for those respective rates. The time reported in the simulations is taken in the unit  $\tau_s = \frac{1}{k_{\text{spread}}}$ . All the simulations in this paper were performed by taking an average over 2000 independent runs.

### III. RESULTS

#### A. Kinetics of modification spreading

##### 1. MMST: Simulations and mean field theory

We simulated the spreading of histone modification as discussed in the Model section for various nucleosome densities computing MMST as a function of sliding rates. The MMST is defined as the time required for the first successful modification of the last nucleosome ( $i = N$ ), given that the modification spreads from the initiation site ( $i = 0$ ). These are similar to the mean first passage time calculations in statistical mechanics [74,75], which are a measure of modification spreading time.

We observed that, as the sliding rate increases, the mean modification spreading time decreases and saturates to a constant value (Fig. 2). For a zero sliding rate, on a sufficiently long DNA, the probability of finding, at least, one pair of nucleosome neighbors with a gap (linker length) greater than 10 bp is very high. Hence, for the zero sliding rate, the modification may not reach the other end implying that MMST can be infinity. In order to see the effect of sliding, the MMST was computed at three different nucleosome densities (90%, 85%, and 80%). Here, the demodification rate  $k_r$  of the nucleosome was kept fixed at 0.01.

We also used a mean-field theoretical study to understand how MMST would vary with sliding rates for different densities. For this calculation at a given density, we have taken nucleosomes to be homogeneously distributed along the lattice. The effect of nucleosome sliding was incorporated in the effective spreading rate of modification  $k_{\text{se}}$ , which is a function of the sliding rate of the nucleosome and average internucleosomal distance. The MMST ( $T_{i \rightarrow n}$ ), from the  $i$ th

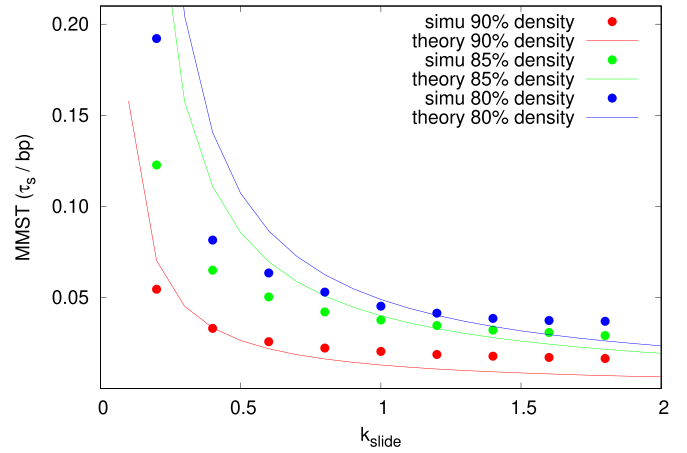


FIG. 2. Quicker sliding reduces the spreading time: The MMST with  $k_{\text{slide}}$  using simulations (simulation, dots) and mean-field theoretical calculations (theory, lines) for different nucleosome densities, viz.—90% (red), 85% (green), and 80% (blue). All rates are measured in units of  $k_{\text{spread}}$

to the  $n$ th nucleosome follows the difference equation [76]:

$$T_{i \rightarrow n} = \frac{1}{k_{\text{se}} + k_r} + \frac{k_{\text{se}}}{k_{\text{se}} + k_r} T_{i+1 \rightarrow n} + \frac{k_r}{k_{\text{se}} + k_r} T_{i-1 \rightarrow n}, \quad (1)$$

where index  $i$  varies from 0 to  $N$ . The index  $i = 0$  represents the nucleation site, whereas 1 and  $N$  are indices of the first and last nucleosome, respectively.  $N$  is the total number of nucleosomes in the model. By solving this  $N + 1$  set of linear equations (see the Appendix)

$$T_{0 \rightarrow N} = \frac{1}{(k_{\text{se}})^N} \sum_{\ell=1}^N (N - \ell + 1) (k_{\text{se}})^{N-\ell} k_r^{\ell-1}. \quad (2)$$

It is expected that when the demodification rate of nucleosomes is set to zero (i.e.,  $k_r = 0$ ), Eq. (2) reduces to  $T_{0 \rightarrow N} = \frac{N}{k_{\text{se}}}$ . In this equation,  $k_{\text{se}}$  depends on the sliding rate of the nucleosome and the internucleosomal distance via the relation [77,78],

$$k_{\text{se}} = \frac{l_s^2 k_{\text{slide}}}{\text{gap}^2}, \quad (3)$$

where  $l_s = 10 \text{ bp}$  is the step size of sliding events, and the gap is the linker length. This relation can be understood as an inverse of the timescale of the meeting of two nucleosomes. In Fig. 2, we plot the mean-field theory results [Eq. (2), curves] along with the simulation results (dots). For certain nucleosome densities, both results are comparable. A significant variation was observed in MMST when the density was varied from 90% to 85%. The higher values of MMST at lower densities are a signature of the presence of long gaps (greater than 10 bp) between nucleosomes, which eventually slows down the spreading of modifications. This also implies that MMST is higher when  $k_{\text{slide}} \ll k_{\text{spread}}$ , whereas it is found to be smaller in the opposite limit.

We have got elevated profiles of MMST at 85% and 80% nucleosome densities, implying reduced densities contribute toward an increase in MMST values. For low sliding rates (less than or around 0.5), the MMST changes a lot with the

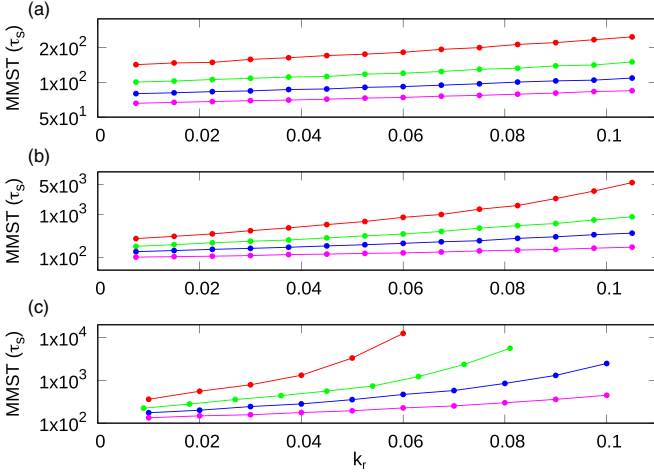


FIG. 3. Spreading time increases with demodification events: The MMST as a function of demodification rate  $k_r$  for different nucleosome densities (a) 90%, (b) 85%, and (c) 80%. The different curves are for sliding rates, 0.5, 1, 2, and 6 from top (red) to bottom (magenta). All rates are measured in units of  $k_{\text{spread}}$ .

sliding rate indicating the longer times it takes to spread the modifications across the lattice. For higher sliding rates, the MMST change is small. Altogether, all these results imply that the sliding of nucleosomes can play a significant role in spreading the modification across the lattice.

## 2. Demodification events increase spreading time

In reality, modified nucleosomes can get demodified, and such demodification events may be crucial in some contexts. To examine the effect of demodification on MMST, we varied the demodification rate ( $k_r$ ) over a range. In Fig. 3, we present our results for MMST on changing the demodification rates of nucleosomes for four different sliding rates: 0.5 (red), 1 (green), 2 (blue), and 6 (magenta). Since the residence time of the modification [47,80] is more than spreading time, we take the demodification rate  $k_r \ll 1$  in units of  $\frac{1}{\tau_s}$ .

In Figs. 3(a), 3(b), and 3(c), MMST results are plotted for different nucleosome densities, 90%, 85%, and 80%, respectively. Here, one sees an interplay between nucleosome demodification rate and sliding rate. An increase in demodification rates contributes to the corresponding increase in the MMST. It would take a longer time for spreading the modification across the lattice for larger values of demodification rates. However, an increase in sliding rates from 0.5 to 6 (red, green, blue, and magenta curves) has contributed to a substantial decrease in the MMST. It was found that with a reduction in nucleosome density, the gaps between nucleosomes as well as demodification rates have contributed to an increase in modification spreading times.

### B. Domains of modified nucleosomes: Effect of sliding and demodification events

In this section, we discuss how the modified domains of nucleosomes are maintained for different sliding and demodification rates at a fixed nucleosome density. We calculated the probability of modified nucleosomes at a steady state. The

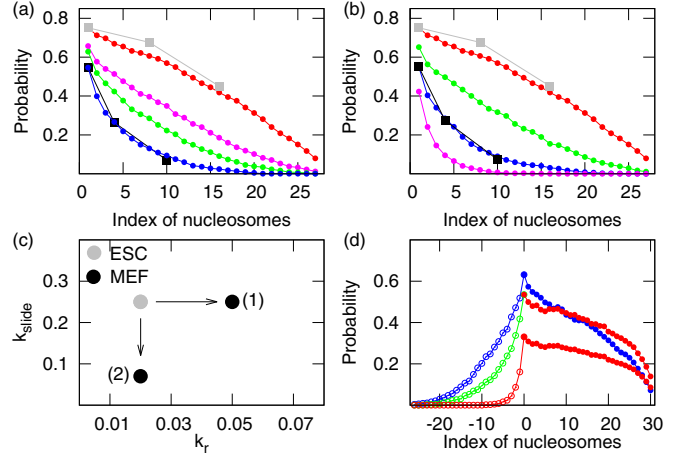


FIG. 4. Quantities with sliding and demodification rates: The probability of modified nucleosomes for sliding and demodification rates at 80% nucleosome density: (a) for  $k_r = 0.02$ ,  $k_{\text{slide}} = 0.25$  (red), 0.15 (magenta), 0.11 (green), and 0.07 (blue) and (b) for  $k_{\text{slide}} = 0.25$ ,  $k_r = 0.02$  (red), 0.03 (green), 0.05 (blue), and 0.1 (magenta). Experimental data (Hathaway *et al.* [45]) for MEF cells is shown by black squares and for embryonic stem (ES) cells by gray squares. (c) Plot of  $k_r$  with  $k_{\text{slide}}$  for MEF and ES cells. Black dots represent pairs of parameters that fit MEF data, whereas the gray dot fits ES data. (d) Probabilities at 80% density (left of initiation site) for  $k_{\text{slide}} = 0.1$  (red), 1 (green), and 2.2 (blue) open circles and 90% density (right of initiation site) for  $k_{\text{slide}} = 0.1$  (red) and 0.075 (blue) filled circles. All times are measured in units of  $\tau_s$ .

simulations were carried out by varying sliding rates whereas fixing  $k_r = 0.02$  [Fig. 4(a)]. The experimental H3K9me3 ChIP data [circles for embryonic stem cells (ESCs) and squares for mouse embryonic fibroblasts (MEFs)] provided in the right part from nucleation site in Fig. 6(d) of Hathaway *et al.* [45] is used for comparison with simulations.

The probability of finding modified nucleosomes at any location along the DNA contour at 80% nucleosome density is depicted in Fig. 4 with different colors representing different sliding and demodification rates. The probability sharply decays as we decrease the sliding rate [Fig. 4(a)]. In other words, the modification pattern tends to get more localized with a peak at the initiation (source) site. This sharp decay in modification profile is similar to what is observed in experiments near the nucleation site. For  $k_{\text{slide}} = 0.07$  and 0.25, our simulation results are comparable to experimental H3K9me3 ChIP data from Hathaway *et al.* [45] of MEFs and ES cells, respectively. A similar set of simulations were repeated at 90% nucleosome density for different sliding rates (see Fig S4-A in the Supplemental Material [79]). In this case, density has played an important role in modification of these nucleosomes along with their sliding rates. A significant decrease in probabilities at the end of lattice is a signature of demodification events dominating over the spreading of modifications.

As a next step, simulations were carried out by varying demodification rates whereas fixing the  $k_{\text{slide}} = 0.25$  [Fig. 4(b)]. For small  $k_r$  values, such as 0.02 and 0.03, the modification pattern has a larger spread. It was found that for  $k_r = 0.02$ , our simulation results are comparable to experimental H3K9me3

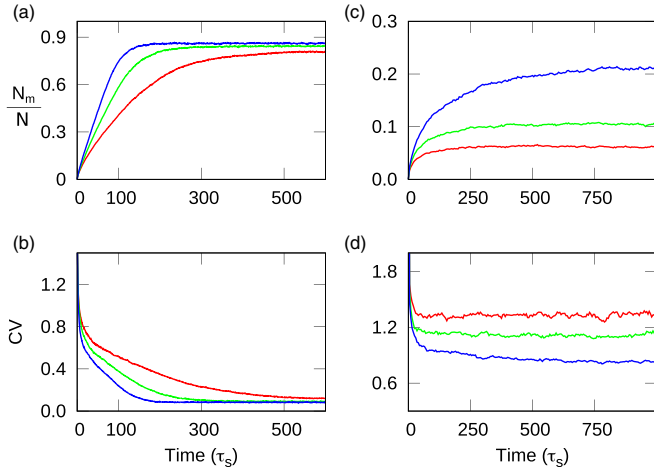


FIG. 5. Statistics of modified nucleosomes: The (a) fraction of modified nucleosomes and (b) coefficient of variation (CV) of modified nucleosomes for 90% nucleosome density ( $N = 31$  nucleosomes), (c) fraction of modified nucleosomes, and (d) CV of modified nucleosomes for 80% nucleosome density ( $N = 27$  nucleosomes). All plots are for different nucleosome sliding rates  $k_{\text{slide}} = 0.5$  (red), 1 (green), and 2 (blue) for lattice length  $L = 5000$  bp. All times are measured in units of  $\tau_s$ .

ChIP data from Hathaway *et al.* [45] of ES cells. For relatively higher  $k_r$  values localized modification pattern is observed with a peak near the initiation site. At  $k_r = 0.05$  the simulated modification profile is comparable to what is observed in experiments for MEF cells. Overall, it is seen that MEF curves are more localized than ES curves near the nucleation site. From our simulations, we find that high  $k_r$  is required to get curves that are localized near nucleation sites. This implies

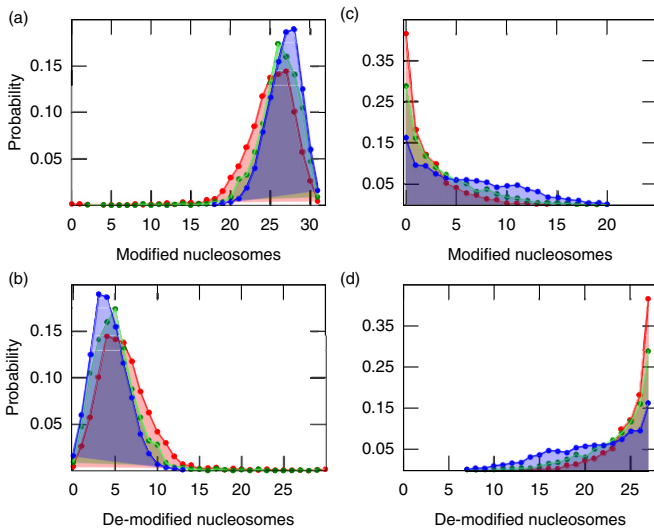


FIG. 6. Number distribution profiles of modified and demodified nucleosomes: The probability distributions of number of (a) modified and (b) demodified nucleosomes at 90% nucleosome density. The probability distributions of number of (c) modified and (d) demodified nucleosomes at 80% nucleosome density for nucleosome sliding rates  $k_{\text{slide}} = 0.5$  (red), 1 (green), and 2 (blue). All rates are measured in units of  $k_{\text{spread}}$ .

that the chromatin state of the MEF has higher modification removal (higher demethylation). On the other hand, in the case of  $k_{\text{slide}}$ , the lower sliding rate will take you from ESC to MEF. This is consistent with the notion that stem cells have more dynamic nucleosomes [81,82].

Figure 4(c) summarizes how changes in parameters  $k_r$  and  $k_{\text{slide}}$  take the cell from ES state to MEF state. Each dot in the plot represents a pair of parameters ( $k_r, k_{\text{slide}}$ ) that fits with the experimental data. These corresponding pairs of parameters are provided in the Supplemental Material Table S1 [79]. We show that we can go from the ES state to the MEF state in multiple ways. A fit to the differentiated MEF data (black dot 1) can be achieved by a 2.5-fold increase in the  $k_r$  value from that of the ES cells (gray dot), whereas keeping the sliding parameter the same. Similarly, a fit to the MEF data (black dot 2) can also be achieved by an approximately 0.35-fold decrease in  $k_{\text{slide}}$  value from that of the ES cells, whereas keeping the  $k_r$  parameter the same. Thus, appropriately changing the  $k_r$  and  $k_{\text{slide}}$  values, we can get the localized MEF curves as reported in Fig. 4.

Our results so far suggest that combinations of different sliding rates and nucleosome densities can lead to very different modification patterns. It is plausible that on either side of certain boundaries or boundary elements (e.g., transcription start site), nucleosome density and the action of chromatin remodelers could be very different. We explored this to examine whether this can lead to an asymmetry in nucleosome modification spread patterns [55]. We simulated nucleosomes with different densities and sliding rates on either side of a boundary (initiation site). The results are in Fig. 4(d), where the asymmetry in the positioning of modified nucleosomes about the initiation site can be seen. The density of the nucleosomes are always fixed at 90% on the right-hand side of the initiation site and at 80% on the left-hand side. Then different combinations of sliding rates are taken on both sides of the initiation site. The top blue curve (with open circles on the left of the initiation site for  $k_{\text{slide}} = 2.2$  and filled circles on the right of the initiation site for  $k_{\text{slide}} = 0.075$ ) has least asymmetry; the bottom red curve (with open circles on the left of the initiation site and filled circles on the right of the initiation site for  $k_{\text{slide}} = 0.1$ ) has maximum asymmetry. Thus, we suggest that variability in sliding rates and nucleosome densities is a potential way of explaining the asymmetry across various boundary elements.

These results together show that the interplay between nucleosome demodification rate and the sliding rate determines the profile of the modification pattern. At low sliding and high demodification rates, the modification peaks near the source and decays quickly. For high sliding rate and low demodification rate, the decay is more gradual.

**C. Dynamics of modified nucleosomes: Estimation of statistical quantities**

In this subsection, we discuss the time evolutions in the amount of modification and its fluctuations at biologically relevant nucleosome densities (80% and 90%). For each time step, we plot the mean fraction of modified nucleosomes  $\frac{N_m}{N}$ , where  $N_m$  is the mean number of modified nucleosomes (Fig. 5). The fluctuations were quantified using the CV, a

dimensionless quantity defined as the ratio of the standard deviation to the mean. These quantities were calculated for different sliding rates  $k_{\text{slide}} = 0.5, 1, 2$ .  $k_r$  was kept fixed at 0.1. At  $t = 0$ ,  $N_m$  is taken as zero. As expected,  $\frac{N_m}{N}$  increases with time and saturates. Here different trajectories (colors) correspond to different rates of sliding. At higher density, the variation in  $\frac{N_m}{N}$  for different sliding rates (i.e., different curves with different colors) is small. However, at lower density (80%), the mean dynamics shows huge variation as we change the sliding rates, suggesting that the steady state as well as the dynamics at low densities are crucially affected by the sliding rates.

We find that CV values decrease as a function of time. This could be because in the beginning the modification numbers are less, and, hence, the fluctuation is high. At 90% density, CV is smaller than unity (standard deviation is smaller than the mean), and CV is similar at the steady state for all sliding rates. However, for 80% nucleosome density, the CVs show well-separated steady states, and fluctuations are comparable or bigger than the mean (CV is comparable or above 1). We found almost the same steady states for a fraction of the modified nucleosomes and CV when the simulation was performed at 80% nucleosome density with all nucleosomes modified ( $N = 27$ ) at  $t = 0$ . This implies that the final states are independent of the initial conditions (whether all nucleosomes or none of them were modified) (see Fig. S1 in the Supplemental Material [79]).

The probability distributions for the number of modified and demodified nucleosomes at 90% and 80% nucleosome densities are depicted in Fig. 6. These distributions were obtained by finding nucleosome numbers at steady states. In Fig. 6(a), for given sliding rates, distributions of modified nucleosomes are negatively skewed. It was found that at 90% density almost all nucleosomes were modified for lower (0.5) and higher (2) values of sliding rates. This implies that, at high nucleosome density, modification is not much affected by sliding rates of nucleosomes. The distribution of demodified nucleosomes is shown in Fig. 6(b). At 80% nucleosome density, in Figs. 6(c) and 6(d), qualitatively similar distributions were observed for low and high values of sliding rates. At a lower sliding rate (0.5), less number of nucleosomes were modified; whereas at a higher sliding rate, modification spreads along the lattice modifying a large number of nucleosomes.

#### D. Relaxation dynamics of modifications when the initiation site is removed

The cell actively maintains the average number of modified nucleosomes by constantly inserting modifications. In this subsection, we examine how the number of modified nucleosomes decreases as a function of time if the nucleation site is removed (i.e., spreading from the nucleation site is switched off). We discuss two different cases. In the first case, at  $t = 0$  all nucleosomes are assumed to be in the modified state. As the time starts, we stop influx of histone modification enzymes from the initiation site ( $k_{\text{recruit}} = 0$ ). That is, starting from a fully modified state, we fixed  $k_{\text{recruit}} = 0$  and simulated dynamics taking all other events. In the second case, we sim-

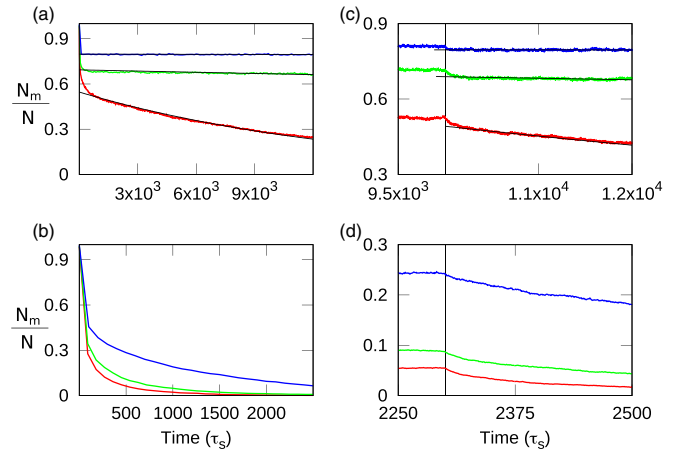


FIG. 7. Relaxation of modified nucleosomes for different sliding rates: The time profiles of a fraction of modified nucleosomes at nucleosome densities (a) 90% ( $N = 31$  nucleosomes) and (b) 85% ( $N = 29$  nucleosomes) when all nucleosomes are modified at  $t = 0$  and  $k_{\text{recruit}} = 0$ . At nucleosome densities (c) 90% and (d) 85% at  $t = 0$ ,  $k_{\text{recruit}} = 1$  and all nucleosomes are unmodified. At steady state (black vertical line) of modification we take  $k_{\text{recruit}} = 0$ . All the results are for sliding rates  $k_{\text{slide}} = 0.1$  (red), 0.2 (green), and 0.5 (blue). The fitted curve is shown in black, and all times are measured in units of  $\tau_s$ .

ulated the full system to obtain the steady state, and at some time point in the steady state, we set  $k_{\text{recruit}} = 0$ .

In Fig. 7(a) we present the results for the first case with higher density (90%) and different nucleosome sliding rates [0.2 (green), 0.5 (blue), and 0.1 (red)]. We observe that stable patterns of modified nucleosomes are maintained for sliding rates 0.2 and 0.5 in the, respective, steady states. However, when the sliding rate is low [0.1 (red)] the fraction of modified nucleosomes decreases as a function of time. This curve was fitted with an exponentially decaying function giving rise to a decay rate of the order of  $10^{-6}$  per unit time. This is analogous to the effective demodification rate in our simulations. The loss of steady-state pattern emphasizes the importance of sliding events even at such a high density. However, at lower densities (85%) in Fig. 7(b), such steady-state patterns are absent for all the sliding rates simulated. However, for the higher sliding rate, the mean modification decays slowly.

In the second case, we simulated the full system (taking all events discussed in subsection III C until the steady state. At a particular time point indicated by the vertical bar in Figs. 7(c) and 7(d), influx of modification was switched off ( $k_{\text{recruit}}$  is set to 0). For higher sliding rates [0.2 (green) and 0.5 (blue)] and higher density, there is no dip in the fraction of modified nucleosomes. However, for a lower sliding rate [0.1 (red)], the fraction of modified nucleosomes decreases a bit but stays near the steady state. At 85% nucleosome density, the fraction of modified nucleosomes decay slightly but stays close to their respective steady states. Fitting the decay curve with an exponential function, the decay constant at 85% nucleosome density is found to be around  $10^{-3}$  per unit time (see Supplemental Material Table S2 and Table S3 [79]).

In short, the interplay between density and sliding decides the relaxation dynamics of modifications; an increase in  $k_{\text{slide}}$

values (from 0.1 to 0.5) slows down the decay of the modified nucleosomes. The sliding of the nucleosome contributes to slowing down the decay (also see supporting information Fig. S2 and Fig. S3 in the Supplemental Material [79]).

#### IV. CONCLUSIONS AND SUGGESTIONS FOR EXPERIMENTS

In this article, we have discussed how nucleosome sliding may affect the spreading of histone modifications along the lattice. The spread of modifications is quantified by estimating the MMST. It was found that for low nucleosomal sliding rates, it takes a longer time for spreading the modification across the lattice; whereas it takes less time for higher sliding rates. We confirmed these findings by performing an analytical estimation of MMST using a mean-field theory. It was also found that the interplay between nucleosome sliding events and nucleosome density determines spreading times. The larger demodification rates contributed to enhanced modification spreading times, but the sliding rates of nucleosomes helped to restrict them. The dynamics of modified nucleosomes were studied by computing statistical quantities, such as fluctuations and probability distributions, which were found to be dependent upon nucleosome densities. We show that for certain densities and sliding rates, the nucleosome modification pattern is localized in a region as seen in experiments. This paper also shows that certain parameters can give rise to the asymmetric nature of nucleosome modifications about the initiation site. The interplay between sliding events and density of nucleosomes also influences the relaxation dynamics of modifications. Overall, the proposed model gives insights into the role of sliding events and how the interplay between density and sliding can be an important determinant.

The main prediction of the paper is how the sliding of nucleosomes and nucleosome densities can influence the spreading of modifications. This can be tested by developing appropriate mutants of nucleosome sliding enzymes and examining whether the mutations affect the spreading of modifications. One may also design different chromatin arrays having very different nucleosome densities (nucleosome repeat lengths) and examine how these would influence the spreading of modifications.

#### ACKNOWLEDGMENTS

This research has been supported by funds to S.K. from the Department of Science and Technology, India under Science and Engineering Research Board, National Postdoctoral Fellowship (NPDF) with File No. PDF/2017/002502 and to R.P. from the Department of Biotechnology, India Grant No. BT/HRD/NBA/39/12/2018-19.

#### APPENDIX: RECURSIVE RELATION OF MEAN FIRST PASSAGE TIME FROM SURVIVAL PROBABILITY

A simplified mean-field calculation of this model can give a closed form expression for MMST as a function of rates. For this calculation, we take nucleosomes homogeneously distributed along the lattice. The modification spreads from the nucleation site with an effective rate  $k_{se}$ , which depends on sliding rate and internucleosomal distance by the following relation [77,78]:

$$k_{se} = \frac{l_s^2 k_{slide}}{gap^2}. \quad (A1)$$

For MMST calculations, we first calculate survival probability  $[S_{i \rightarrow n}(t)]$ , which is defined as: The probability that modification has not reached the  $n$ th nucleosome until time  $t$ , given that at  $t = 0$ th nucleosome was already modified [76],

$$\frac{\partial S_{i \rightarrow n}(t)}{\partial t} = k_{se} S_{i+1 \rightarrow n}(t) + k_r S_{i-1 \rightarrow n} - (k_{se} + k_r) S_{i \rightarrow n}(t). \quad (A2)$$

We can write first passage time  $T_{i \rightarrow n}$  as

$$T_{i \rightarrow n} = \int_0^\infty t F_{i \rightarrow n}(t) dt = \int_0^\infty t \frac{-\partial S_{i \rightarrow n}(t)}{\partial t} dt \\ = -t S_{i \rightarrow n}(t) \Big|_0^\infty - \int_0^\infty 1 \cdot [-S_{i \rightarrow n}(t)] dt \quad (A3)$$

$$= \int_0^\infty S_{i \rightarrow n}(t) dt. \quad (A4)$$

The first term in Eq. (A3) vanishes because for any bounded survival probability at long time is  $\approx 0$ , and it approaches zero much faster than  $1/t$ ,

$$\int_0^\infty \frac{\partial S_{i \rightarrow n}(t)}{\partial t} dt = k_{se} \int_0^\infty S_{i+1 \rightarrow n}(t) dt + k_r \int_0^\infty S_{i-1 \rightarrow n} dt - (k_{se} + k_r) \int_0^\infty S_{i \rightarrow n}(t) dt, \quad (A5)$$

$$S_{i \rightarrow n}(\infty) - S_{i \rightarrow n}(0) = k_{se} T_{i+1 \rightarrow n} + k_r T_{i-1 \rightarrow n} - (k_{se} + k_r) T_{i \rightarrow n}$$

$$T_{i \rightarrow n} = \frac{1}{k_{se} + k_r} + \frac{k_r}{k_{se} + k_r} T_{i-1 \rightarrow n} + \frac{k_{se}}{k_{se} + k_r} T_{i+1 \rightarrow n}. \quad (A6)$$

In Eq. (A5)), we have used two properties of survival probability that a system should survive with probability 1 at  $t = 0$  and modification should survive with probability  $\approx 0$  at a very long time.

Now using Eq. (A6), we can write a recursive equation between MMSTs: ( $T_{i \rightarrow N} \rightarrow$  MMST from the  $i$ th nucleosome to the  $N$ th nucleosome),

$$T_{0 \rightarrow N} = \frac{1}{k_{recruit}} + T_{1 \rightarrow N}, \quad T_{1 \rightarrow N} = \frac{1}{k_{se} + k_r} + \frac{k_{se}}{k_{se} + k_r} T_{2 \rightarrow N} + \frac{k_r}{k_{se} + k_r} T_{0 \rightarrow N}, \\ T_{2 \rightarrow N} = \frac{1}{k_{se} + k_r} + \frac{k_{se}}{k_{se} + k_r} T_{3 \rightarrow N} + \frac{k_r}{k_{se} + k_r} T_{1 \rightarrow N},$$

$$\begin{aligned}
& \vdots \\
& \vdots \\
& \vdots \\
T_{i \rightarrow N} &= \frac{1}{k_{se} + k_r} + \frac{k_{se}}{k_{se} + k_r} T_{i+1 \rightarrow N} + \frac{k_r}{k_{se} + k_r} T_{i-1 \rightarrow N}, \\
& \vdots \\
& \vdots \\
T_{N-1 \rightarrow N} &= \frac{1}{k_{se} + k_r} + \frac{k_{vr}}{k_{se} + k_r} T_{N-2 \rightarrow N}, \\
T_{N \rightarrow N} &= 0.
\end{aligned} \tag{A7}$$

We can write these equations in matrix form,

$$\mathbb{M}T = B,$$

$$\begin{bmatrix}
k_{\text{recruit}} & -k_{\text{recruit}} & & & 0 \\
-k_r & k_{se} + k_r & -k_{se} & \cdots & \cdots \\
0 & \cdots & \cdots & \cdots & \cdots \\
& & & & \\
& & & & \\
& & & & \\
0 & \cdots & -k_r & k_{se} + k_r & -k_{se} \\
& & & -k_r & k_{se} + k_r
\end{bmatrix}
\begin{bmatrix}
T_{0 \rightarrow N} \\
T_{1 \rightarrow N} \\
\vdots \\
\vdots \\
\vdots \\
T_{N-2 \rightarrow N} \\
T_{N-1 \rightarrow N}
\end{bmatrix}
=
\begin{bmatrix}
1 \\
1 \\
\vdots \\
\vdots \\
\vdots \\
1 \\
1
\end{bmatrix}. \tag{A8}$$

$k_{\text{recruit}}$  and  $k_{se}$  are function of nucleosome density and  $k_{\text{slide}}$ . We solve the above equation by taking inverse of matrix  $\mathbb{M}$  to get  $T_{1 \rightarrow N}$ . For simplicity first take  $k_{\text{recruit}} = k_{se}$ ,

$$T_{0 \rightarrow N} = \frac{1}{(k_{se})^N} \sum_{\ell=1}^N (N - \ell + 1) k_{se}^{N-\ell} k_r^{\ell-1}. \tag{A9}$$

- 
- [1] B. Alberts, *Molecular Biology of the Cell 5E* (Garland Science, New York, 2008).
- [2] K. E. Van Holde, *Chromatin* (Springer, Berlin, 2012).
- [3] R. D. Kornberg, *Science* **184**, 868 (1974).
- [4] R. Cortini, M. Barbi, B. R. Caré, C. Lavelle, A. Lesne, J. Mozziconacci, and J.-M. Victor, *Rev. Mod. Phys.* **88**, 025002 (2016).
- [5] N. Kaplan, I. K. Moore, Y. Fondufe-Mittendorf, A. J. Gossett, D. Tillo, Y. Field, E. M. LeProust, T. R. Hughes, J. D. Lieb, J. Widom *et al.*, *Nature (London)* **458**, 362 (2009).
- [6] K. Brogaard, L. Xi, J.-P. Wang, and J. Widom, *Nature (London)* **486**, 496 (2012).
- [7] T. Raveh-Sadka, M. Levo, U. Shabi, B. Shany, L. Keren, M. Lotan-Pompan, D. Zeevi, E. Sharon, A. Weinberger, and E. Segal, *Nat. Genet.* **44**, 743 (2012).
- [8] P. Milani, G. Chevereau, C. Vaillant, B. Audit, Z. Hafteker-Terreau, M. Marilley, P. Bouvet, F. Argoul, and A. Arneodo, *Proc. Natl. Acad. Sci. USA.* **106**, 22257 (2009).
- [9] Z. Zhang, C. J. Wippo, M. Wal, E. Ward, P. Korber, and B. F. Pugh, *Science* **332**, 977 (2011).
- [10] R. D. Kornberg and L. Stryer, *Nucleic Acids Res.* **16**, 6677 (1988).
- [11] R. Padinhateeri and J. F. Marko, *Proc. Natl. Acad. Sci. USA.* **108**, 7799 (2011).
- [12] J. J. Parmar, J. F. Marko, and R. Padinhateeri, *Nucleic Acids Res.* **42**, 128 (2014).
- [13] V. B. Teif and K. Rippe, *Nucleic Acids Res.* **37**, 5641 (2009).
- [14] T. van der Heijden, J. J. van Vugt, C. Logie, and J. van Noort, *Proc. Natl. Acad. Sci. USA.* **109**, E2514 (2012).
- [15] A. V. Morozov, K. Fortney, D. A. Gaykalova, V. M. Studitsky, J. Widom, and E. D. Siggia, *Nucleic Acids Res.* **37**, 4707 (2009).
- [16] R. V. Chereji, S. Ramachandran, T. D. Bryson, and S. Henikoff, *Genome Biol.* **19**, 19 (2018).
- [17] Z. Jiang and B. Zhang, *Phys. Rev. Lett.* **123**, 208102 (2019).
- [18] Z. Jiang and B. Zhang, *PLoS Comput. Biol.* **17**, e1008556 (2021).
- [19] V. B. Teif, *Briefings Bioinf.* **17**, 745 (2016).
- [20] V. B. Teif and C. T. Clarkson, *Encyclop. Bioinform. Comput. Biol.* **2**, 308 (2019).
- [21] T. Bameta, D. Das, and R. Padinhateeri, *Nucleic Acids Res.* **46**, 4991 (2018).
- [22] D. K. Pokholok, C. T. Harbison, S. Levine, M. Cole, N. M. Hannett, T. I. Lee, G. W. Bell, K. Walker, P. A. Rolfe, E. Herbolsheimer *et al.*, *Cell* **122**, 517 (2005).
- [23] W.-H. Lien, X. Guo, L. Polak, L. N. Lawton, R. A. Young, D. Zheng, and E. Fuchs, *Cell Stem Cell* **9**, 219 (2011).
- [24] F. Erdel, *BioEssays* **39**, 1700053 (2017).

- [25] C. D. Allis, T. Jenuwein, and D. Reinberg, *Epigenetics* (Cold Spring Harbor Laboratory Press, New York, 2007).
- [26] S. Ramachandran and S. Henikoff, *Sci. Adv.* **1**, e1500587 (2015).
- [27] R. Margueron, N. Justin, K. Ohno, M. L. Sharpe, J. Son, W. J. Drury Iii, P. Voigt, S. R. Martin, W. R. Taylor, V. De Marco *et al.*, *Nature (London)* **461**, 762 (2009).
- [28] R. Bonasio, S. Tu, and D. Reinberg, *Science* **330**, 612 (2010).
- [29] B. Zhang, X. Wu, W. Zhang, W. Shen, Q. Sun, K. Liu, Y. Zhang, Q. Wang, Y. Li, A. Meng *et al.*, *Mol. Cell* **72**, 673 (2018).
- [30] L. C. Lindeman, C. L. Winata, H. Aanes, S. Mathavan, P. Aleström, and P. Collas, *Int. J. Dev. Biol.* **54**, 803 (2010).
- [31] Y. Hayashi-Takanaka, K. Yamagata, N. Nozaki, and H. Kimura, *J. Cell Biol.* **187**, 781 (2009).
- [32] Y. Hayashi-Takanaka, K. Yamagata, T. Wakayama, T. J. Stasevich, T. Kainuma, T. Tsurimoto, M. Tachibana, Y. Shinkai, H. Kurumizaka, N. Nozaki *et al.*, *Nucleic Acids Res.* **39**, 6475 (2011).
- [33] Y. Sato, L. Hilbert, H. Oda, Y. Wan, J. M. Heddleston, T.-L. Chew, V. Ziburdaev, P. Keller, T. Lionnet, N. Vastenhouw *et al.*, *Development* **146**, dev179127 (2019).
- [34] I. M. Hall, G. D. Shankaranarayana, K.-i. Noma, N. Ayoub, A. Cohen, and S. I. Grewal, *Science* **297**, 2232 (2002).
- [35] G. Schotta, A. Ebert, V. Krauss, A. Fischer, J. Hoffmann, S. Rea, T. Jenuwein, R. Dorn, and G. Reuter, *EMBO J.* **21**, 1121 (2002).
- [36] G. Felsenfeld and M. Groudine, *Nature (London)* **421**, 448 (2003).
- [37] K. Zhang, K. Mosch, W. Fischle, and S. I. Grewal, *Nat. Struct. Mol. Biol.* **15**, 381 (2008).
- [38] R. C. Allshire and H. D. Madhani, *Nat. Rev. Mol. Cell Biol.* **19**, 229 (2018).
- [39] A. Buscaino, E. Lejeune, P. Audergon, G. Hamilton, A. Pidoux, and R. C. Allshire, *EMBO J.* **32**, 1250 (2013).
- [40] T. Zhang, S. Cooper, and N. Brockdorff, *EMBO Rep.* **16**, 1467 (2015).
- [41] I. B. Dodd, M. A. Micheelsen, K. Sneppen, and G. Thon, *Cell* **129**, 813 (2007).
- [42] K. Sneppen, M. A. Micheelsen, and I. B. Dodd, *Mol. Syst. Biol.* **4**, 182 (2008).
- [43] I. B. Dodd and K. Sneppen, *J. Mol. Biol.* **414**, 624 (2011).
- [44] M. J. Obersriebnig, E. M. H. Pallesen, K. Sneppen, A. Trusina, and G. Thon, *Nat. Commun.* **7**, 11518 (2016).
- [45] N. A. Hathaway, O. Bell, C. Hodges, E. L. Miller, D. S. Neel, and G. R. Crabtree, *Cell* **149**, 1447 (2012).
- [46] C. Hodges and G. R. Crabtree, *Proc. Natl. Acad. Sci. USA.* **109**, 13296 (2012).
- [47] L. C. Anink-Groenen, T. R. Maarleveld, P. J. Verschure, and F. J. Bruggeman, *Epigenet. Chromatin* **7**, 30 (2014).
- [48] M. Ancona, D. Michieletto, and D. Marenduzzo, *Phys. Rev. E* **101**, 042408 (2020).
- [49] H. Zhang, X.-J. Tian, A. Mukhopadhyay, K. S. Kim, and J. Xing, *Phys. Rev. Lett.* **112**, 068101 (2014).
- [50] H. Binder, L. Steiner, T. Rohlf, S. Prohaska, and J. Galle, *Nat. Preced.*, 1 (2011).
- [51] F. Erdel and E. C. Greene, *Proc. Natl. Acad. Sci. USA.* **113**, E4180 (2016).
- [52] D. Michieletto, E. Orlandini, and D. Marenduzzo, *Phys. Rev. X* **6**, 041047 (2016).
- [53] D. Jost and C. Vaillant, *Nucleic Acids Res.* **46**, 2252 (2018).
- [54] S. H. Sandholtz, B. G. Beltran, and A. J. Spakowitz, *J. Phys. A: Math. Theor.* **52**, 434001 (2019).
- [55] S. H. Sandholtz, D. Kannan, B. G. Beltran, and A. J. Spakowitz, *Biophys. J.* **119**, 1630 (2020).
- [56] S. H. Sandholtz, Q. MacPherson, and A. J. Spakowitz, *Proc. Natl. Acad. Sci. USA.* **117**, 20423 (2020).
- [57] M. Katava, G. Shi, and D. Thirumalai, *Biophys. J.* **121**, 2895 (2022).
- [58] H. J. Szerlong and J. C. Hansen, *Biochem. Cell Biol.* **89**, 24 (2011).
- [59] J. Bednar, R. A. Horowitz, S. A. Grigoryev, L. M. Carruthers, J. C. Hansen, A. J. Koster, and C. L. Woodcock, *Proc. Natl. Acad. Sci. USA.* **95**, 14173 (1998).
- [60] G. J. Narlikar, R. Sundaramoorthy, and T. Owen-Hughes, *Cell* **154**, 490 (2013).
- [61] C. Y. Zhou, S. L. Johnson, N. I. Gamarra, and G. J. Narlikar, *Annu. Rev. Biophys.* **45**, 153 (2016).
- [62] L. Mollazadeh-Beidokhti, F. Mohammad-Rafiee, and H. Schiessel, *Biophys. J.* **96**, 4387 (2009).
- [63] R. Blossey and H. Schiessel, *FEBS J.* **278**, 3619 (2011).
- [64] A.-M. Florescu, H. Schiessel, and R. Blossey, *Phys. Rev. Lett.* **109**, 118103 (2012).
- [65] R. Murugan, *Biophys. J.* **114**, 2516 (2018).
- [66] R. Schwanbeck, H. Xiao, and C. Wu, *J. Biol. Chem.* **279**, 39933 (2004).
- [67] E. Segal, Y. Fondufe-Mittendorf, L. Chen, A. Thåström, Y. Field, I. K. Moore, J.-P. Z. Wang, and J. Widom, *Nature (London)* **442**, 772 (2006).
- [68] H. Schiessel, J. Widom, R. F. Bruinsma, and W. M. Gelbart, *Phys. Rev. Lett.* **86**, 4414 (2001).
- [69] S. G. Swygert and C. L. Peterson, *Biochim. Biophys. Acta Gene. Regul. Mech.* **1839**, 728 (2014).
- [70] J. L. Doob, *Trans. Am. Math. Soc.* **52**, 37 (1942).
- [71] J. L. Doob, *Trans. Am. Math. Soc.* **58**, 455 (1945).
- [72] D. Gillespie, *J. Comput. Phys.* **22**, 403 (1976).
- [73] D. Gillespie, *J. Phys. Chem.* **81**, 2340 (1977).
- [74] S. Redner, *A Guide to First-Passage Processes* (Cambridge University Press, Cambridge, UK, 2001).
- [75] R. Murugan, *J. Phys. A* **39**, 1575 (2006).
- [76] C. W. Gardiner, *Handbook of Stochastic Methods* (Springer, Berlin, 1985), Vol. 3.
- [77] V. Balakrishnan and M. Khantha, *Pramana* **21**, 187 (1983).
- [78] M. Khantha and V. Balakrishnan, *Pramana* **21**, 111 (1983).
- [79] See Supplemental Material at <http://link.aps.org/supplemental/10.1103/PhysRevE.106.024408> for pairs of parameters.
- [80] R. D. Phair, P. Scaffidi, C. Elbi, J. Vecerová, A. Dey, K. Ozato, D. T. Brown, G. Hager, M. Bustin, and T. Misteli, *Mol. Cell Biol.* **24**, 6393 (2004).
- [81] J. Yu, C. Xiong, B. Zhuo, Z. Wen, J. Shen, C. Liu, L. Chang, K. Wang, M. Wang, C. Wu *et al.*, *Cell Rep.* **32**, 107953 (2020).
- [82] A. van der Velde, K. Fan, J. Tsuji, J. E. Moore, M. J. Purcaro, H. E. Pratt, and Z. Weng, *Commun. Biol.* **4**, 239 (2021).